INSTITUTE OF PLASMA PHYSICS

NAGOYA UNIVERSITY

Determination of metastable fraction in an ion beam extracted from ECR plasma

Atsushi Matsumoto, Shunsuke Ohtani

and Tsuruji Iwai*

(Received - Feb. 9, 1982)

IPPJ - 580 Apr. 1982

RESEARCH REPORT

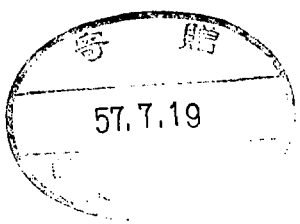

NAGOYA, JAPAN

Determination of metastable fraction in an ion beam extracted from ECR plasma

Atsushi Matsumoto, Shunsuke Ohtani
and Tsuruji Iwai*

(Received - Feb. 9, 1982)

IPPJ - 580 Apr. 1982

---

* Permanent Address; Department of Liberal Arts, Kansai Medical University, Hirakata, Osaka 573, Japan

Abstract

The fraction of metastable-state $Ar^{2+}(3p^4\ ^1D)$ ions in Ar^{2+} beam has been determined by an optical attenuation method (OAM) combined with the conventional beam attenuation method. The present OAM is based on observation of spatial decay of specified emission line intensities arising from charge-changed ions, along the beam axis in a target gas cell. The validity of the OAM is discussed in detail. The cross sections for one-electron capture by the ground-state $Ar^{2+}(^3P)$ ions, σ_{21}, and by the metastable-state $Ar^{2+}(^1D)$ ions, σ^*_{21}, from Na have been measured independently by the OAM. Both the cross sections are of the order of 10^{-14} cm^2 and σ^*_{21} is about 1.3 times as large as σ_{21} at the collision energy of 1.5 keV.

1. Introduction

An ion or atomic beam used in atomic collision experiments, in general, contains a significant fraction of metastable species which depends strongly on the condition of ion production. There have been many examples that in charge-changing collisions the cross sections observed by different investigators are remarkably different owing to different fractions of metastable species in the primary beam used (Massey and Gilbody 1974). Therefore, several techniques have been developed in order to determine and control the metastable fraction of the primary beam (Gilbody 1978). Apart from the fundamental interest, charge-changing collision processes involving multicharged metastable ions are important for the study of high-temperature plasmas.

A beam attenuation method has been developed to obtain the fraction of metastable species in the primary beam and to determine the cross sections for both the ground and the metastable states involved (Turner et al 1968, Gilbody et al 1968), and then the method has been mostly conventional. However, when the charge-changing cross sections would have nearly the same values for ions in the ground state and in the metastable state, as expected for the one-electron capture process by multicharged ions (Salzborn and Müller 1980), the beam attenuation method can hardly be applied. Furthermore, the metastable fraction obtained from the attenuation curve may be different from the true fraction because of excitation and deexcitation processes (Vujović et al 1972, Pedersen 1979).

Seim et al (1981) have proposed another method in which metastable ions are detected through a single subsequent charge-changing collisions. Hollstein et al (1969) studied spectroscopically the collisional deexcitation of He atoms involving the metastable He (2^1S, 2^3S) atoms. Similar approaches have been done by other authors (Blair et al 1973, McCullough et al 1973).

In the present paper, we are concerned with the one-electron capture process by Ar^{2+} ions from Na atom, $Ar^{2+} + Na \rightarrow Ar^{+} + Na^{+}$, at keV collision energies. We propose here an optical attenuation method (OAM) to determine the cross sections of the one-electron capture by Ar^{2+} ions in the metastable ($3p^4\ ^1D$) state as well as in the ground ($3p^4\ ^3P$) state (Matsumoto et al 1981); the present OAM is similar to the spectroscopic study of metastable He atoms by Hollstein et al (1969). In contrast to the beam attenuation method, the OAM is based upon observation of the attenuation of intensities, along the primary beam axis, of specified emission lines from the charge-changed Ar^{+} ions. In spite of spectroscopic measurements, the present OAM needs only relative measurements of emission intensities. Thus, the OAM is rather simple and does not include serious errors associated with the absolute measurement. When the OAM is combined with the beam attenuation method, it gives the fraction of the metastable $Ar^{2+}(3p^4\ ^1D)$ ions in the primary ion beam.

2. Principle of the present method

2-1 Assumptions

The primary $Ar^{2+}(3p^4)$ ion beam is expected to contain the ground-state ^3P ions and the two metastable-state ^1D and ^1S ions. The OAM proposed here is based upon the following assumptions. First, in the one-electron capture process, $Ar^+(3p^4[^3P]nl)$, i.e. $Ar^+(nl)$, ions come only from the ground-state $Ar^{2+}(3p^4\ ^3P)$ ions; $Ar^+(3p^4[^1D]nl)$, i.e. $Ar^+(nl')$, ions come only from the metastable-state $Ar^{2+}(3p^4\ ^1D)$ ions, and $Ar^+(3p^4[^1S]nl)$, i.e. $Ar^+(nl")$, ions come only from the other metastable-state $Ar^{2+}(3p^4\ ^1S)$ ions:

$$Ar^{2+}(^3P) + Na \rightarrow Ar^+(nl) + Na^+, \qquad (1)$$

$$Ar^{2+}(^1D) + Na \rightarrow Ar^+(nl') + Na^+, \qquad (2)$$

and

$$Ar^{2+}(^1S) + Na \rightarrow Ar^+(nl") + Na^+, \qquad (3)$$

In other words, we assume that the state of core configuration of the primary ions does not change during the electron capture collision at keV collision energies. This assumption has been motived by the previous investigation (Matsumoto et al 1980b). It predicts relative population distribution among the possible terms of $Ar^+(4p)$ or $Ar^+(4p')$ state from the statistics based upon the building-up principle of molecule under the radial coupling scheme. If the primary ion is assumed to be in its ground-state ^3P, the measured population

distribution for $Ar^+(4p)$ state is very close to the predicted one, but the measured one for $Ar^+(4p')$ state is quite different at keV collision energies. On the other hand, if the primary ion is assumed to be in its metastable-state ^1D, the measured distribution for $Ar^+(4p')$ is well explained by the statistical model. These fact can be evidence to support the first assumption and its validity is now verified by the present experiment as described in section 4.

Second, we neglect the existence of $Ar^{2+}(^1S)$ ion in the primary beam, because of its probably rather small fraction. In fact, we have never observed the reaction (3) in our previous study. Therefore, we assume that the primary beam consists of the two components $Ar^{2+}(^3P)$ and (^1D) ions hereafter. Third, we assume that each component attenuates independently in passing through a collision cell, that is, the cross sections for exitation and deexcitation processes, $Ar^{2+}(^3P) + Na \rightleftarrows Ar^{2+}(^1D) + Na$, are negligibly small. This assumption is discussed later. Fourth, we assume that the one-electron capture process predominates over such other processes as two-electron capture and charge-stripping. The two-electron capture process is an endothermic reaction more than 9 eV, and the charge-stripping cross section would be very small in the present collision energy range. Therefore, the fourth assumption is reasonably accepted.

2-2 Determination of one-electron capture cross sections by the OAM

The primary Ar^{2+} ion beam attenuates continuously along the beam axis, traversing the sodium target cell. On the above assumptions, the beam intensity of the ground-state $Ar^{2+}(^3P)$ ions, i(x), and that of the metastable-state $Ar^{2+}(^1D)$ ions, i'(x), at a position x along the beam axis in the cell are expressed by

$$i(x) = I_0(1-f)\exp(-\sigma_{21}Nx), \tag{4}$$

and

$$i'(x) = I_0 f \exp(-\sigma^*_{21}Nx), \tag{5}$$

where I_0 is the initial intensity of the primary ion beam, f the fraction of the metastable ^1D ions in the primary ion beam, N the target sodium density, and σ_{21} and σ^*_{21} are the one-electron capture cross sections by the ground-state $Ar^{2+}(^3P)$ ions and the metastable-state $Ar^{2+}(^1D)$ ions, respectively.

The quantities of i(x) and i'(x) can not be measured directly, but these are closely related to the intensities of emission lines coming from the Ar^+(nl) state and from the Ar^+(nl') state at the position x, respectively. If the lifetimes of Ar^+(nl and nl') states are very short, i(x) and i'(x) should be proportional to the intensities of emission lines from the Ar^+(nl) state, S(x), and that from the Ar^+(nl') state, S'(x). Then we have

$$S(x) \propto Q(nl)\ N\ I_0(1-f)\exp(-\sigma_{21}Nx), \tag{4a}$$

and

$$S'(x) \propto Q(nl')\ N\ I_0 f\ \exp(-\sigma^*_{21}Nx), \tag{5a}$$

where Q(nl) and Q(nl') are the cross sections of electron capture into the Ar^+ excited states nl and nl'. Therefore, σ_{21} and σ^*_{21} can be determined independently from the slopes of semilogarithmic plot of S(x) and S'(x) against Nx, if S(x) and S'(x) are measured as a function of x along the beam axis:

$$\ln S(x) = -\sigma_{21}Nx + \text{constant}, \tag{6}$$

and

$$\ln S'(x) = -\sigma^*_{21}Nx + \text{constant}. \tag{7}$$

This is the basis of the present OAM. The lifetime effect mentioned above is discussed later.

2-3 Determination of metastable fraction

Passing through the target cell, the Ar^{2+} ion beam attenuates as follows:

$$I/I_0 = (1-f)\ \exp(-\sigma_{21}NL) + f\ \exp(-\sigma^*_{21}NL), \tag{8}$$

where NL is the target thickness, L the collision length, and I the intensity of the attenuated Ar^{2+} beam. If the cross sections σ_{21} and σ^*_{21} are obtained from the OAM, the fraction of the metastable $Ar^{2+}(^1D)$ ions in the primary beam can be

determined from equation (8) with measurements of I/I_0 as a function of the target thickness.

According to the conventional attenuation method, both the fraction and each cross section are determined from the semilogarithmic plot of I/I_0 as a function of the target thickness. If σ_{21} and σ^*_{21} are nearly the same, however, the conventional method gives neither the fraction nor each cross section; only an apparent cross section is determined. Meanwhile, in the present method, the cross sections σ_{21} and σ^*_{21} are determined from the OAM separately, and fraction can be determined in principle in the case just mentioned above.

3 Experimental procedure and errors

The ion source used in this experiment has been described in detail previously (Matsumoto et al 1979). Ions are produced in an ECR plasma, which is based on electron cyclotron resonance (ECR) heating of plasma in a magnetic bottle. The mirror field was produced with a set of solenoids; the mirror ratio and the field strength at the mirror throat could be varied from 3 to 10 and from 1 to 2 kG, respectively. A microwave power was fed into a discharge chamber through a waveguide (a few kW, 2.45 GHz). A floating electrode with a hole of 2 mm in diameter was placed at the mirror throat. This electrode separated the discharge region from a stage of beam extraction, where the pressure was maintained below 5×10^{-7} Torr. The microwave discharge was operated under a continuous mode at $1\sim2\times10^{-5}$ Torr. Ions extracted from the hole were accelerated to a desired energy. An ion beam, formed after passing through electrostatic lenses and deflectors, was mass-analysed with a 60° sector magnet of 10 cm-radius and injected into a collision chamber.

The present experimental arrangement is schematically shown in figure 1. The ion beam was well collimated by three beam-defining apertures A_1, A_2, and A_3 (A_3: 0.7 mm in diameter) and led into a target cell. The cell is an oven containing sodium vapor (20 mm in length; entrance aperture of 1.0 mm in diameter; exit aperture of 1.5 mm in diameter); the temperature of the cell was measured with a thermocouple. The cell has an orifice at its upside for monitoring the target density and

has a side window made of sapphire. After passing through the cell, ions were charge-separated with a parallel plate deflector just behind the cell. The primary Ar^{2+} and charge-changed Ar^{+} ions were detected with a Faraday cup B having an aperture of 8×12 mm^2. Another Faraday cup A having the same aperture as B was placed at a distance of 16 cm from the cell. This Faraday cup was used to monitor the total ion current. The two Faraday cups were separated by 24 mm.

The target cell was kept at temperatures higher than the part of sodium reservoir to prevent the sapphire window from any contamination of sodium. The sodium atomic beam effusing from the orifice was monitored with a surface ionization detector (tungsten ribbon filament). Calibration of the detector was made by a deposition method; the effusing sodium atoms were condensed on a collector plate attached to the beam shutter cooled by running water; an amount of sodium deposited on the collector plate during several tens of hours was measured in the same manner as that of the previous experiment (Matsumoto et al 1980a). Then the target density is derived from the measured intensity of effusing sodium beam, the temperature of the cell, and the present geometrical dimensions.

The present optical attenuation technique is illustrated in figure 2. The light emission through the window was observed at a right angle to the beam axis. The optical image of emission was focussed on the entrance slit of a monochromator by the use of a condensing lens made of quartz-CaF_2. By sliding the lens parallel to the beam axis, the emission intensity can be observed as a function of the position along

the beam axis. Intensities of specified emission lines were received by a grating monochromator equipped with a photomultiplier (HTV R585S). The light signals were measured by a single-photon-counting system. Typical photon signals were about 100 cps at the primary ion current of several nA, whereas the dark noise count was less than 2 cps. In order to eliminate errors due to fluctuations in the ion current and to reduce random errors of the photon counts, a current integration of the primary beam was made by the use of a voltage-to-frequency converter and a preset counter. The photon signals S(x) and S'(x) were accumulated during the preset interval.

The cross sections σ_{21} and σ^*_{21} are derived from the slope of ln S(x) and ln S'(x) plotted as a function of Nx. Then the error in the cross section value should be the sum of errors in N and in x and random errors coming from the determination of the slope. The estimated uncertainty in the measured target density is similar to that reported previously; errors in the value of N arise mainly from the calibration of the surface ionisation detector and were estimated less than $\pm$ 10 % for the absolute measurement and $\pm$ 2 % for the relative measurement. As for the determination of the position coordinate x by optical measurements, errors come mainly from the magnification of optical image focussed with the condensing lens. This error was estimated less than $\pm$ 0.5 %. Random errors arising from the determination of the slope of ln S(x) and ln S'(x) were estimated at $\pm$ 2.5 %. Then the total error in the cross sections σ_{21} and σ^*_{21} was estimated to be about $\pm$ 11 % in quadrature sum. The error in the ratio $\sigma^*_{21}/\sigma_{21}$,

however, is only due to random errors of the slope determination, because the photon signals S(x) and S'(x) were obtained under the same experimental condition, and therefore the error in the ratio was estimated at $\pm$ 4 %.

Attenuation of the primary ion beam I/I_0 is related to the measured quantities as follows:

$$\frac{I}{I_0} = \frac{I_2/2}{I_1 + I_2/2} , \qquad (9)$$

where I_1 and I_2 are the ion beam currents of singly and doubly charged ions, respectively. A secondary process, $Ar^{2+} + Na \rightarrow Ar^{+} + Na^{+}$ followed by $Ar^{+} + Na \rightarrow Ar + Na^{+}$, was neglected here because of its small cross section (Matsumoto et al 1980a). Both the ion currents I_1 and I_2 were measured with the Faraday cup B; peaks of both the ion currents observed by scanning the applied voltage of the deflector were flat-topped and completely separated from each other; the values of I_1 and I_2 were determined from the heights of these peaks.

As the fraction of the metastable-state ^1D ions in the primary ion beam is determined from equation (8), the error in the fraction value is related to all the measured quantities, I/I_0, σ_{21}, σ^*_{21}, N, and L, in which the errors in the cross section and in the target density have estimated above. Uncertainty of the beam current measurement was within $\pm$ 3 %. Thus the error in the beam attenuation I/I_0 is less than $\pm$ 4.5 %. The effective length L of the gas cell was determined by gas kinematics; the effective length is 1.02 times as large as the geometrical length of the cell.

The error due to this correction may not exceed $\pm$ 2 %. The total error in the fraction f is not a simple sum of errors in the measured quantities, because it is related not only to the error in each quantity measured but also to the value of the measured quantity itself. As a result of rather complicated calculations, the total error in the fraction f was estimated to be $\pm$ 55 % in quadrature sum for the present experiment.

4. Results and discussion

Many emission lines mostly coming from the charge-changed Ar^+(4p, 4d, 5s, and 4p') ions were observed along the primary ion beam axis. Among these lines, two strong emission lines, 3729 A ($4p\ ^4S_{3/2} \rightarrow 4s\ ^4P_{5/2}$) and 4348 A ($4p\ ^4D_{7/2} \rightarrow 4s\ ^4P_{5/2}$), were selected as the representatives of emission lines from the Ar^+(nl) state. The attenuation of emission intensities of the two lines along the beam axis, S(x), is shown in figure 3 (a) as a function of Nx at the collision energy of 1.5 keV. In figure 3 (b) is shown similar attenuation of emission intensities, S'(x), of two lines, 4072 A ($4p'\ ^2D_{5/2} \rightarrow 4s'\ ^2D_{5/2}$) and 4609 A ($4p'\ ^2F_{7/2} \rightarrow 4s'\ ^2D_{5/2}$), at the same collision energy; these lines are the representatives of emission lines from the Ar^+(nl') state.

Three effects at least should be taken into account for the evaluation of S(x) and S'(x). The first is the lifetime effect; fast exited particles such as Ar^+(4p and 4p') ions radiate downstream dependently on their lifetime and velocity. The second is non-uniformity of the target density in the cell; the density should be low near the entrance and exit apertures due to effusion of sodium atoms. The third is concerned with the present geometry of optics; near the ends of the cell, the photon flux received by the present optics is reduced. These effects are enhanced near the end region, and the correction for the effects is necessary there. In fact, the measured photon signals S(x) and S'(x) decrease near the entrance aperture. In the present data shown in figure 3, however,

all the data points measured near the ends of the cell are omitted in order to avoid systematic errors associated with the correction.

As seen in figure 3, the data points line up on the respective single straight lines in the semilogarithmic plot of S(x) and S'(x) versus Nx for all the emission lines observed within experimental errors. This means that the attenuation of each emission intensity is a single exponential decay. If the excitation and deexcitation processes, $Ar^{2+}(^3P) + Na \rightleftarrows Ar^{2+}(^1D) + Na$, would be significant, such a simple decay should not be observed. Therefore, the third assumption in section 2-1 is acceptable for the present experiment.

Furthermore, the slopes of ln S(x) agree with each other for the two emission lines coming from the $Ar^+(4p)$ state within experimental errors; the slope is independent of emission lines observed, if they come from the same $Ar^+(4p)$ state. Quite similarly, the two slopes of ln S'(x) agree with each other; the slope is also independent of emission lines, as far as they come from the same $Ar^+(4p')$ state. These facts can be naturally understood, only when the first assumption is accepted together with the third assumption. That is to say, both the components $Ar^{2+}(^3P)$ and $Ar^{2+}(^1D)$ in the primary ion beam should attenuate independently in traversing the cell, and the state of core configuration of each component, ^3P and ^1D, should not change during the present collision.

As expected from equations (6) and (7), the slopes of ln S(x) and ln S'(x) versus Nx give the cross sections of the one-electron capture by the ground-state $Ar^{2+}(^3P)$ ions σ_{21} and

by the metastable-state $Ar^{2+}(^1D)$ ions σ^*_{21} from Na. These cross sections obtained at the collision energy of 1.5 keV are as follows:

$$\sigma_{21} = (1.34 \pm 0.15)\times 10^{-14} \text{ cm}^2,$$

and

$$\sigma^*_{21} = (1.77 \pm 0.20)\times 10^{-14} \text{ cm}^2.$$

The cross section for the metastable-state ion is about 1.3 times as large as that for the ground-state ion. Such a difference between the slopes for the two components ^3P and ^1D is clearly seen in figure 4, where the data points for the 4348 A emission line are shifted to fit in those for the 3729 A line (both the lines come from the same $Ar^+(4p)$ state) and the data points for the 4609 A line in those for the 4072 A line (both the lines come from the same $Ar^+(4p')$ state).

Figure 5 illustrates the beam attenuation of Ar^{2+} ions I/I_0 measured as a function of the target density at the collision energy of 1.5 keV. Each data point at a fixed target density is the average for several, repeated scans of the deflector voltage. Owing to a rather small difference between σ_{21} and σ^*_{21} observed, the beam attenuation I/I_0 looks like a single exponential decay. As we have just evaluated each value of σ_{21} and σ^*_{21} from the OAM, we can now estimate the fraction of the metastable-state $Ar^{2+}(^1D)$ ions in the primary ion beam. Actually, for every measurement of I/I_0, the corresponding f value was derived from equation (8), and then these f values obtained were averaged out. The mean

value of the fraction f obtained in such a way is estimated to be (0.29 ± 0.16). Though we can not say definitely about the fraction value because of its rather large error, it is noted that the fraction f=0.29 obtained here is close to the statistical composition of the ^1D ions in the primary Ar^{2+} (^3P, ^1D, and ^1S) ion beam. According to our previous work under a single-collision condition, the ratio of the emission intensity of the 3729 A line coming from the $Ar^+(4p)$ state to that of the 4072 A line from the $Ar^+(4p')$ state was independen of such parameters of the ECR ion source as the pressure, the magnetic field and its mirror ratio, and the microwave power at keV collisions within experimental errors. This fact suggests that the metastable fraction is independent of the present ion source parameters.

5. Concluding remarks

The cross sections of the one-electron capture by the ground-state $Ar^{2+}(^3P)$ ions, σ_{21}, and by the metastable-state $Ar^{2+}(^1D)$ ions, σ^*_{21}, from Na have been determined independently by the optical attenuation method (OAM). Both the cross sections measured are of the order of 10^{-14} cm^2 and the value of σ^*_{21} is about 1.3 times as large as that of σ_{21} at the collision energy of 1.5 keV. In combination with the conventional beam attenuation method, the OAM gives the fraction of the metastable-state ^1D ions in the primary Ar^{2+} ion beam. The fraction is estimated at around 29 %, which is close to the statistical composition of the ^1D ions among the $Ar^{2+}(^3P, ^1D,$ and $^1S)$ ions.

The present OAM has two merit at least. First, it offers a useful means for determination of σ_{21} and σ^*_{21}, in particular, in case σ_{21} is nearly the same as σ^*_{21}, because it is able to determine each cross section independently. Second, in spite of spectroscopic measurements, the OAM does not need absolute measurements of emission intensities. Therefore, the OAM is rather simple and does not include serious errors associated with absolute measurements. This merit is very important for the study in the VUV region. Quite recently, Brazuk and Winter (1982) successfully applied the modified OAM in the VUV region to the $(Ne^{2+} + Xe)$ collision system. Furthermore, only relative measurement of the target density is necessary for determining the metastable ion fraction, when the OAM is combined with the beam attenuation method. This may be another merit.

Care should be taken, however, on applying the OAM, because it is based on several assumptions, of which validity has been checked by the present experiment and from the statistical consideration described in our previous paper. Among these assumptions, the first assumption is most important; it is assumed that the state of core configuration of the primary ions is conserved during the one-elecron capture collision. Such an assumption can not be acceptable for violent collisions. At keV energy collisions involving multicharged ions, however, there may be a number of one-elecron transfer collision systems where this assumption is reasonably accepted.

Acknowledgments

The authors would like to thank Mr. T Hino and Dr. H Maezawa for their assistance in constructing the apparatus. Thanks are also due to Professor M Otsuka for his encouragement.

This work was done under the Collaborating Research Program at Institute of Plasma Physics, Nagoya University and supported in part by the Grant-in-Aid for Special Research No. 510508 from the Ministry of Education.

References

Blair W G F, McCullough R W, Simpson F R and Gilbody H B 1973 J. Phys. B: Atom. Molec. Phys. 6 1265-76

Brazuk A and Winter H 1982 to be published in J. Phys. B: Atom. Molec. Phys.

Gilbody H B, Browning R and Levy G 1968 J. Phys. B: Atom. Molec. Phys. 1 230-2

Gilbody H B 1978 Inst. Phys. Conf. Ser. No. 38 156-68

Hollstein M, Sheridan J R, Peterson J R and Lorents D C 1969 Phys. Rev. 187 118-22

Massey H S W and Gilbody H B 1974 Electronic and Ionic Impact Phenomena vol. 4 (Oxford: Clarendon Press) pp. 2707-12

Matsumoto A, Aihara S, Ohtani S, Okuno K, Tsurubuchi S, Iwai T and Kaneko Y 1979 IPPJ-380, Research Report, Institute of Plasma Physics, Nagoya University

Matsumoto A, Tsurubuchi S, Iwai T, Ohtani S, Okuno K and Kaneko Y 1980a J. Phys. Soc. Japan 48 567-74

——1980b J. Phys. Soc. Japan 48 575-82

Matsumoto A, Maezawa H, Ohtani S and Iwai T 1981 Proc. 12th Int. Conf. on Electronic and Atomic Collisions, Gatlinburg pp. 644-5

McCullough R W, Simpson F R and Gilbody H B 1973 J. Phys. B: Atom. Molec. Phys. 6 L322-5

Pedersen E H 1979 Phys. Rev. Lett. 42 440-3

Salzborn E and Müller A 1980 Proc. 11th Int. Conf. on Electronic and Atomic Collisions, Kyoto ed. Oda N and Takayanagi K (North-Holland) Invited papers and progress reports pp. 407-26

Seim W, Müller A and Salzborn E 1981 Z. Phys. A: Atoms and Nuclei 301 11-6

Turner B R, Rutherford J A and Compton D M J 1968 J. Chem. Phys. 48 1602-8

Vujović M, Matić M, Čobić B and Gordeev Yu S 1972 J. Phys. B: Atom. Molec. Phys. 5 2085-97

Figure captions

figure 1. Schematic view of the present experimental setup

figure 2. Schematic diagram of the optical attenuation method

figure 3. Attenuation of emission intensities versus Nx.
(a), 3729 A line and 4348 A line from Ar^+(4p) state
(b), 4072 A line and 4609 A line from Ar^+(4p') stat

figure 4. Comparison between attenuations of emission intensities coming from Ar^+(4p) and Ar^+(4p') states. open circles are data points for 3729 A line and 4072 A line; solid circles for 4348 A line and 4609 A line (see text for detail).

figure 5. Attenuation of Ar^{2+} ion beam intensity

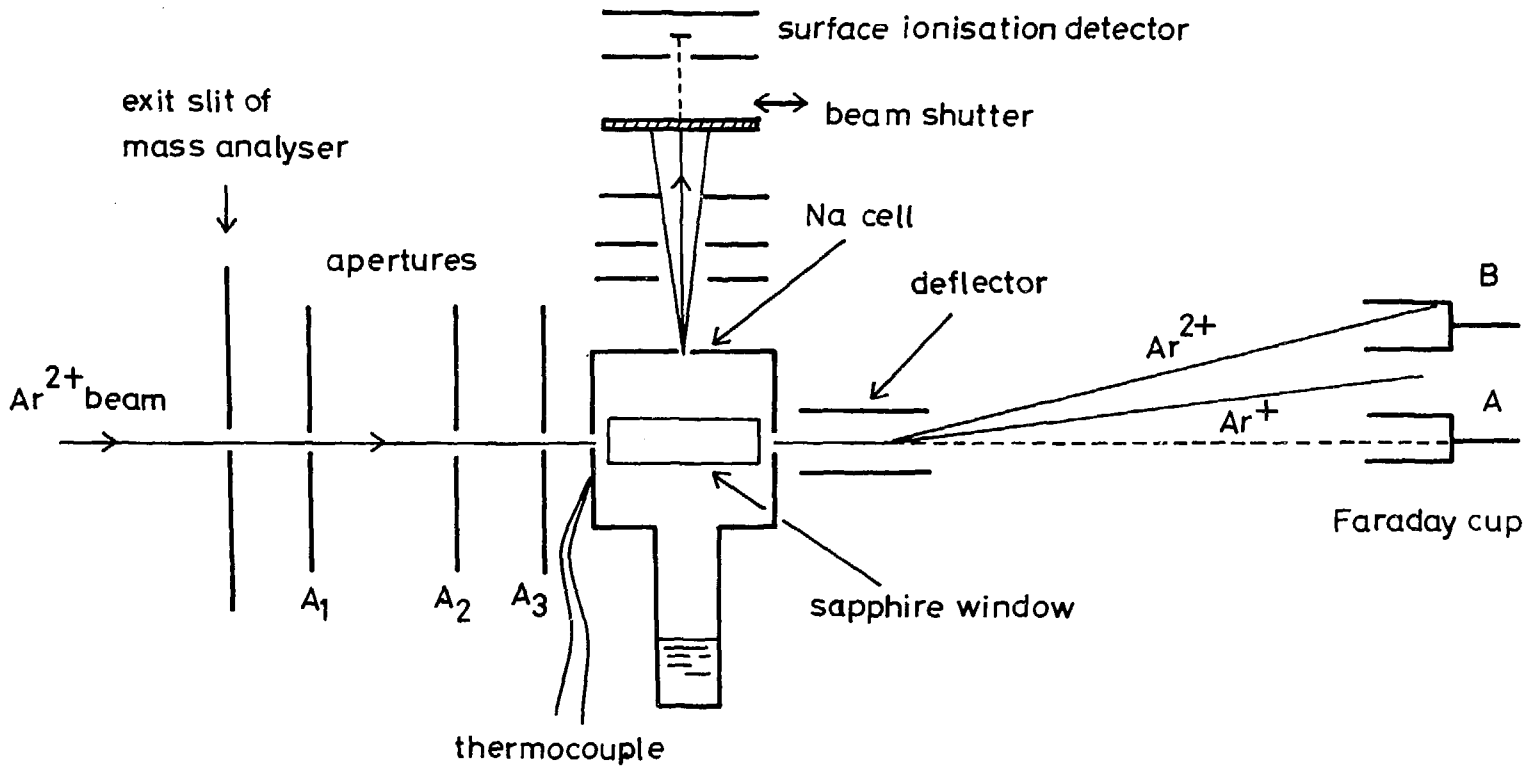
surface ionisation detector
exit slit of
mass analyser
beam shutter
Na cell
apertures
deflector
B
Ar^{2+} beam
Ar^{2+}
Ar^{+}
A
Faraday cup
A_1
A_2
A_3
sapphire window
thermocouple

Fig. 1

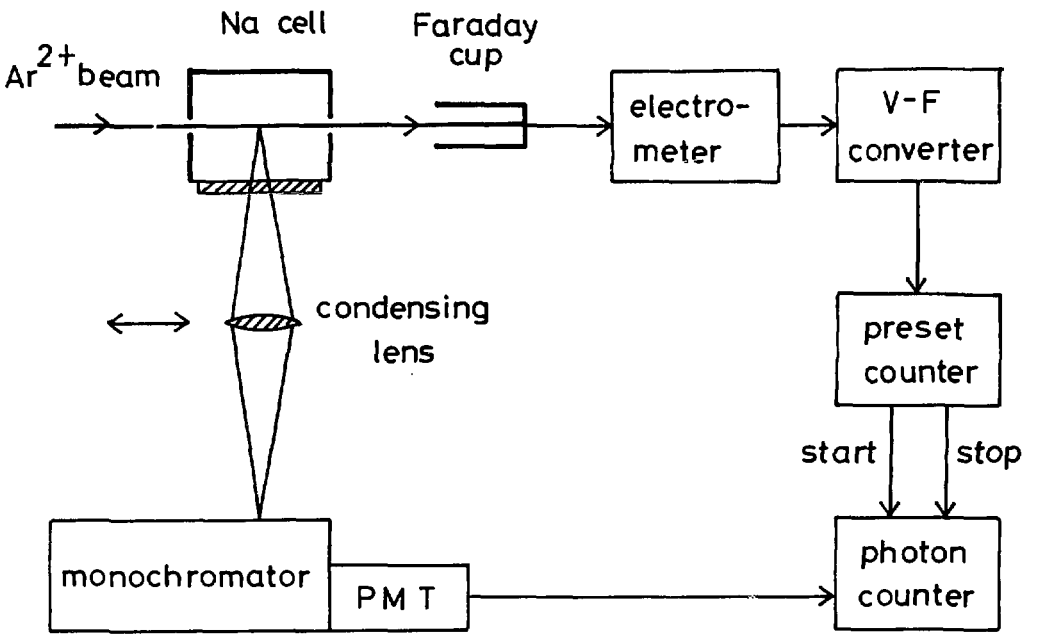
Na cell
Faraday cup
Ar^{2+} beam
electro-meter
V-F converter
condensing lens
preset counter
start
stop
monochromator
PMT
photon counter

Fig. 2

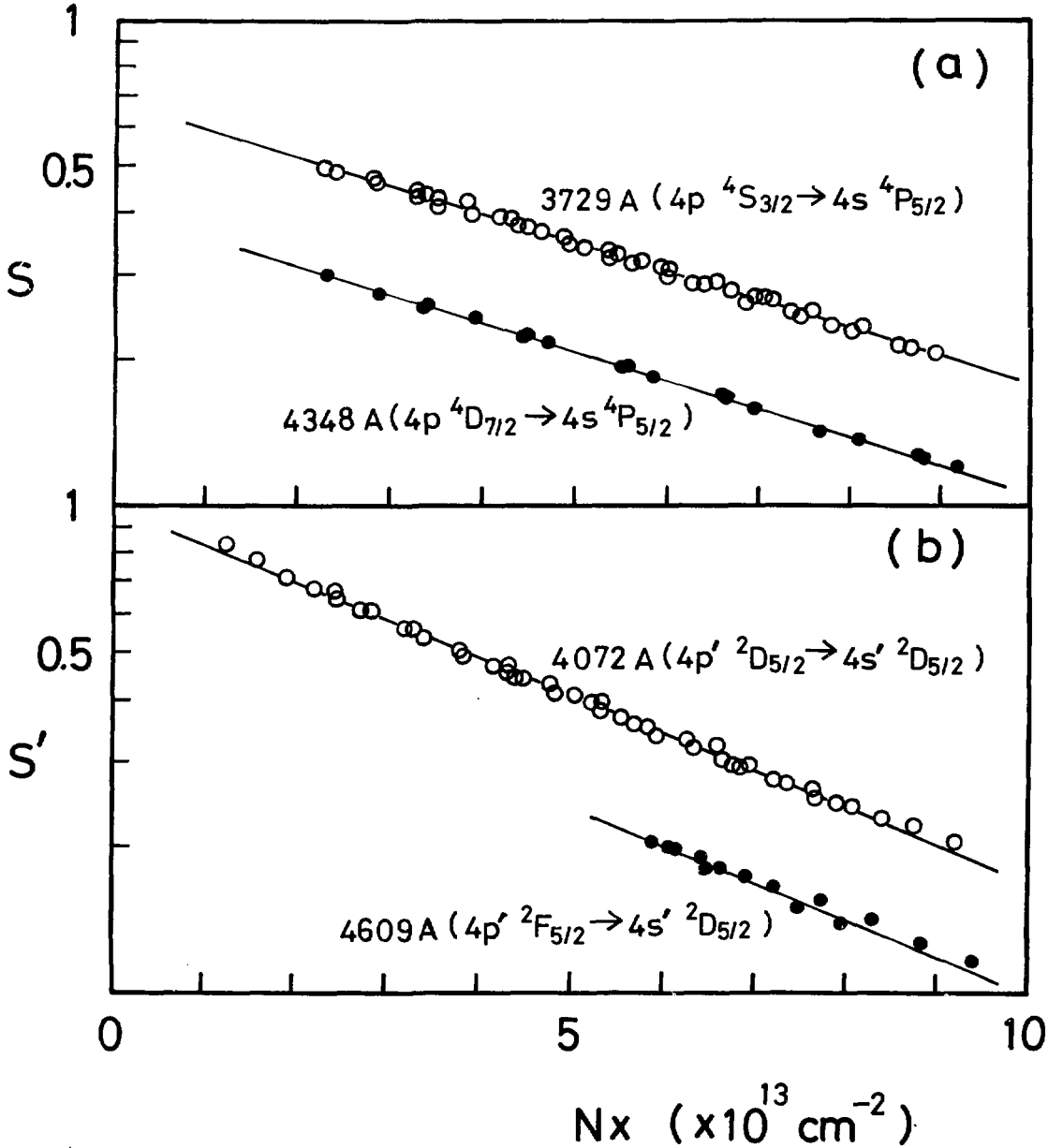
(a)
3729 A (4p $^4S_{3/2}$ → 4s $^4P_{5/2}$)
4348 A (4p $^4D_{7/2}$ → 4s $^4P_{5/2}$)
S
1
0.5
1
(b)
4072 A (4p' $^2D_{5/2}$ → 4s' $^2D_{5/2}$)
4609 A (4p' $^2F_{5/2}$ → 4s' $^2D_{5/2}$)
S'
0.5
0
5
10
Nx (x10^{13} cm^{-2})

Fig. 3

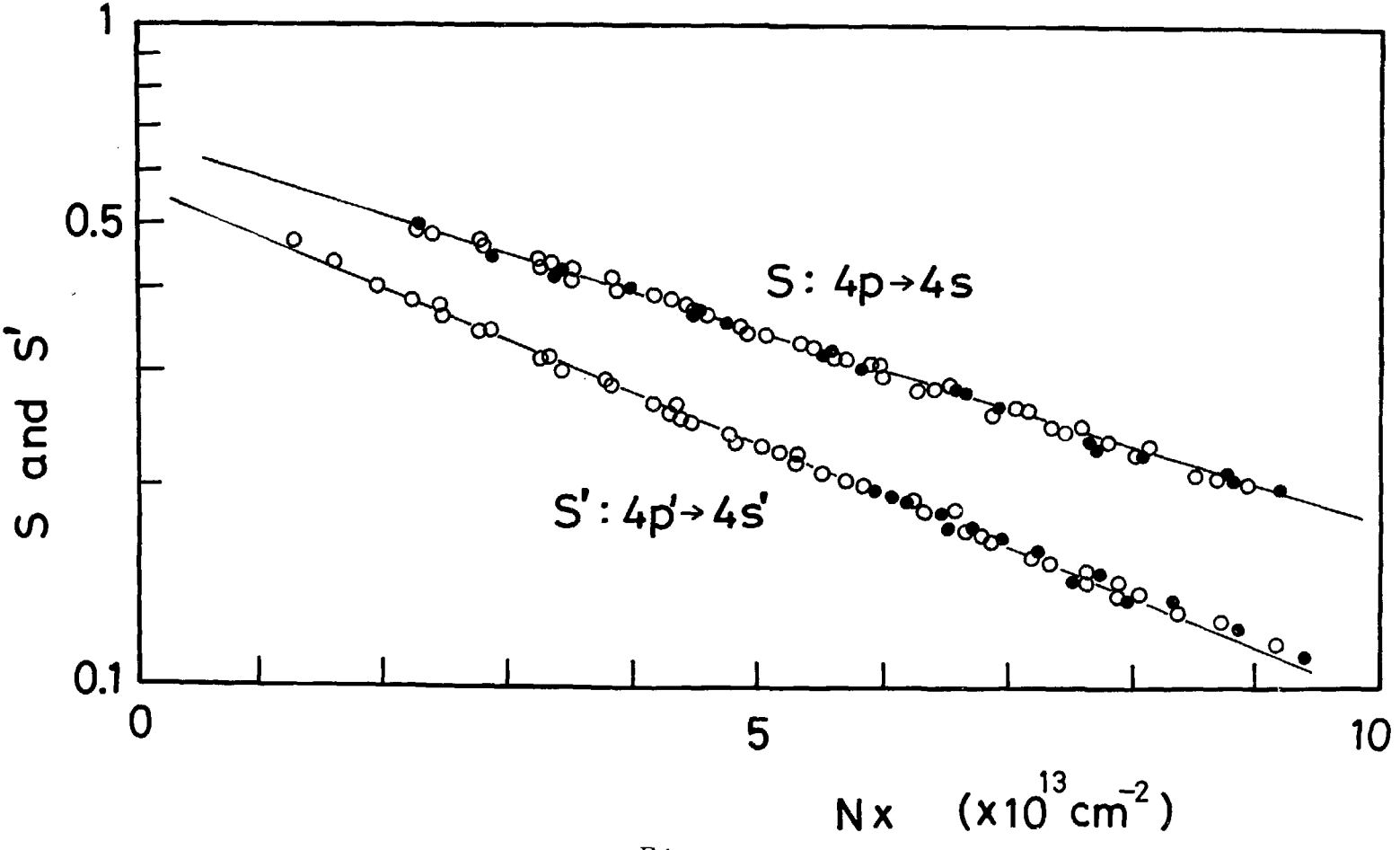

Fig. 4

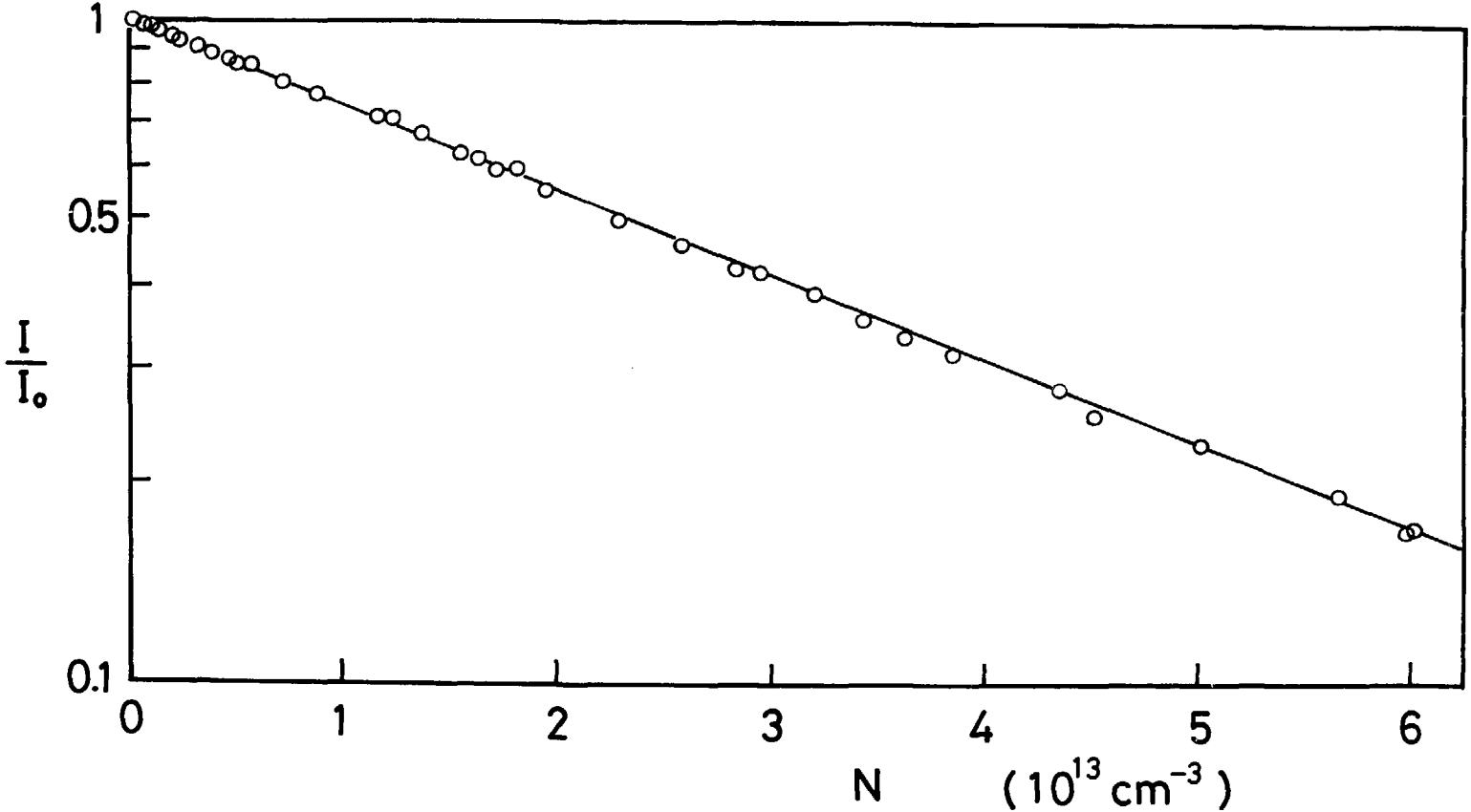

Fig. 5